Numerical Simulations of a Rocket Engine Internal Flow

Conference Paper *in* Journal of the Brazilian Society of Mechanical Sciences and Engineering · November 2018

DOI: 10.26678/ABCM.ENCIT2018.CIT18-0785

5 authors, including:

Luan Lamon Machado
Instituto Federal de Educação, Ciência e Tecnologia do Espírito Santo (IFES)
7 PUBLICATIONS **0** CITATIONS
SEE PROFILE

Leandro Fernandes
Instituto Federal de Educação, Ciência e Tecnologia do Espírito Santo (IFES)
7 PUBLICATIONS **6** CITATIONS
SEE PROFILE

Marcio Teixeira de Mendonca
Instituto de Aeronáutica e Espaço
60 PUBLICATIONS **145** CITATIONS
SEE PROFILE

ENCIT 2018

ABCM Associação Brasileira de Engenharia e Ciências Mecânicas

17th Brazilian Congress of Thermal Sciences and Engineering
November 25th-28th, 2018, Águas de Lindóia, SP, Brazil

NUMERICAL SIMULATIONS OF A ROCKET ENGINE INTERNAL FLOW

Luan Lamon Machado
Saionara Coelho Peixoto
Leandro Marochio Fernandes
Roberto Guilherme Lopes
Instituto Federal de Educação, Ciência e Tecnologia, Cachoeiro de Itapemirim, ES, 29300-970, Brazil
luanlamon@hotmail.com, saionarapeixoto@hotmail.com, leandro.mfernandes@ifes.edu.br, robertoglopes@hotmail.com

Márcio Teixeira de Mendonça
Instituto de Aeronáutica e Espaço, São José dos Campos, SP, 12228-904, Brazil
marcio_tm@yahoo.com

Abstract. *The present work studies the compressible flow of an ideal gas in a convergent-divergent nozzle of a 200 N thrust rocket engine to determine the flow proprieties and its characteristics. The work focuses on a numeric study making use of the Finite Volume Method to approximate the Navier-Stokes equations. Among the used tools, Gmsh stands out for the geometric model reproduction and the nozzle's hexagonal mesh formulation. For the modelling of the problem, and solution of it, the OpenFoam was used. Three situations were studied: subsonic flow regime, supersonic with the presence of normal shock waves and the design point condition.*

Keywords: *Finite Volume Method, Shock Waves, OpenFoam, Numerical Analysis*

1. INTRODUCTION

Understand the complex phenomena involved in Thermal-Fluid Sciences is extremely important when one wishes to study different areas of engineering, i.e., from the analysis of blood flow applied to biomechanics, the understanding of the movement of air mass observed in meteorology, to the various concepts of aerodynamics such as the lift and drag. There is a serie of effects that add up, making it difficult to understand a certain application.

One way to get around this apparent difficulty is to study the simplest cases and follow through with studies until arriving at more complex mechanisms. Following this line of reasoning, the present paper focuses on the numerical study of a compressible flow in a 200N thrust rocket engine nozzle specified by Salvador (2005).

The de Laval-Nozzle, so-called as convergent-divergent, or CD nozzle is a mechanical device used in rocket engines to convert thermal energy from combustion products, allowing the exhaust gases to reach speeds higher than the input, reaching supersonic speeds. The high kinetic energy of the flow results in a large thrust (Anderson, 2001).

The determination of flow characteristics in a CD nozzle can be performed experimentally, analytically or through a computational analysis, used here to obtain a prediction of flow behavior based on compressible Navier-Stokes equations solved by computational fluid dynamics (CFD) in association with equation to state to relate the thermodynamic variables and close the system (Anderson, 1990).

Since the compressible flow in a rocket engine nozzle is extremely difficult to be solved analytically, and the costs involved in the search for an experimental solution are very high, it is evident the need to use computational resources to solve the equations to obtain an approximate result, with a small and controlled margin of error.

For the simulations in the present study, the open source OpenFoam package will be used. OpenFoam was written in $C++$ and based on the Finite Volume Method. From this it will be possible to analyze the Laval nozzle compressible flow, and verify the phenomena involved therein, and to obtain a design curve.

2. NUMERICAL METHOD

A nozzle model specified by Salvador (2005) was used in the implementation of CFD modeling for evaluation of performance and optimization of compressible flows (Fig. 1). The modeling involved a pré-processing step to 2D geometry reproduction in a hexagonal mesh.

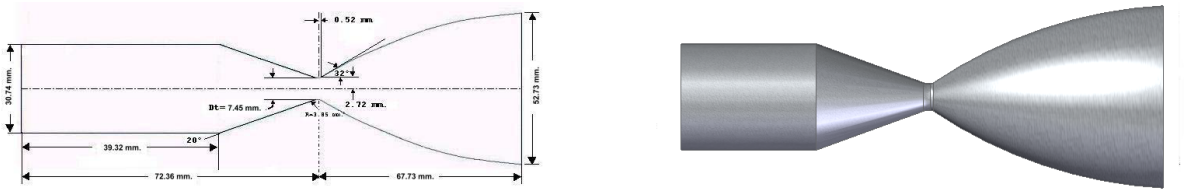

(a) The Laval nozzle nozzle dimensions. (b) The model reproduced.

Figure 1. Schematic drawing of the $200N$ thrust rocket engine (Salvador, 2005).

A mesh convergence study was performed to ensure a smooth transition between the elements and to avoid numerical diffusion (Lantz *et al.*, 1971). Subsequently a specific comparison between different meshes showed that the increase in the number of elements improves the precision of the numerical method (Fernandes *et al.*, 2012). Also, in the study it was found that the hexagonal grid is necessary because it provides a better structural alignment of the mesh in relation a directional flow, conform Fig. 2 (Fernandes, 2012).

```
82  /*******************************************************************
83   *    Convertendo a malha de não-estruturada para estruturada      *
84   *******************************************************************/
85  // Para a câmara
86  Line Loop(20) = {2, 3, 6, 1};
87  Plane Surface(21) = {20};
88  Transfinite Line {2, 3} = 20 Using Progression 1
89  Transfinite Line {1, 6} = 35 Using Progression 1
90  // Força a malha a conter triângulos estruturado
91  Transfinite Surface {21} = {1, 2, 4, 3};
92  //combina triângulos com quadrangulos
93  Recombine Surface {21};
94
95  // Para a convergente
96  Line Loop(22) = {4, 7, 5, -6};
97  Plane Surface(23) = {22};
98  Transfinite Line {4, 5} = 40 Using Bump 0.95;
99  Transfinite Line {6, 7} = 35 Using Progression 1
100 Transfinite Surface {23} = {3, 4, 6, 5};
101 Recombine Surface {23};
```

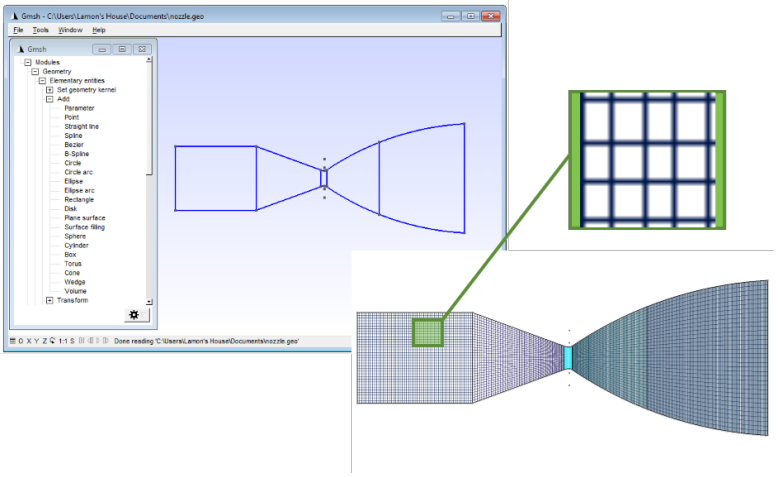

Figure 2. Structured mesh used with GMSH.

Once the problem physics has been identified, fluid properties, flow physics model, and boundary conditions were set. To solve the CD nozzle internal flow a computational analyse is implemented in OpenFoam source code. A *rhoCentralFoam* solver algorithms based on the Gudonov Riemann (Godunov, 1959) method was performed to predict the appearance of the shock wave (Einfeldt, 1988), (Freitas, 2014) and (Gupta, 2016).

The following boundary conditions were specified in OpenFoam. For the pressure, the *totalPressure* boundary condition was admitted at the inlet surface of the CD nozzle. In the nozzle output, a boundary condition *waveTransmissive* was used to avoid reflection of waves within the domain. As initial condition, a constant pressure equal to the outlet pressure is assumed. As the initial condition, a *constant pressure* equal to the outlet pressure is assumed. For the temperature, the Newman boundary condition *zeroGradient* was used for all surfaces. For the initial condition, a constant ambient temperature were specified. For speed, the *zeroGradient* condition was adopted at the inlet and outlet of the nozzle, while on the walls the *slip* condition was admitted, i.e., there is no friction of the fluid with the nozzle structure. Initially the velocity field is constant.

Since OpenFoam only works in the three-dimensional field, the *empty* condition for all properties was adopted to simulate a 2D flow.

3. RESULTS

The numerical delineation begins in the analysis of the mesh quality. From Fig.3 it can be seen that the mesh meets the quality criteria.

```
    inlet              34       70       ok (non-closed singly connected)
    outlet             34       70       ok (non-closed singly connected)

Checking geometry...
    Overall domain bounding box (-72.36 -26.36 0) (67.73 26.36 1)
    Mesh (non-empty, non-wedge) directions (1 1 0)
    Mesh (non-empty) directions (1 1 0)
    All edges aligned with or perpendicular to non-empty directions.
    Boundary openness (-1.97320971162261e-19 -1.57856776929809e-18 2.0193905748990
8e-18) OK.
    Max cell openness = 2.20897975156659e-16 OK.
    Max aspect ratio = 14.3290816482636 OK.
    Minimum face area = 0.065192684070541. Maximum face area = 1.5505882352995.  F
ace area magnitudes OK.
    Min volume = 0.065192684070541. Max volume = 0.692310958686826.  Total volume
= 4312.77954577117.  Cell volumes OK.
    Mesh non-orthogonality Max: 32.9271356356764 average: 9.95001388750805
    Non-orthogonality check OK.
    Face pyramids OK.
    Max skewness = 1.01356262450049 OK.
    Coupled point location match (average 0) OK.

Mesh OK.
```

Figure 3. Convergence of the numerical method.

Two meshes were analyzed: one with 8160 hexahedral elements, and another more refined containing 11560 elements. Metrics such as orthogonality of the elements, aspect ratio and skewness were analyzed (Fig.3). Although both presented optimum quality, the 11560 element mesh represented more accurately the pressure variation and other internal flow properties (Fig. 4).

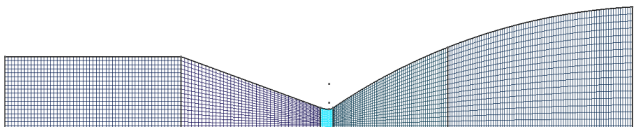

(a) Mesh with 8160 elements.

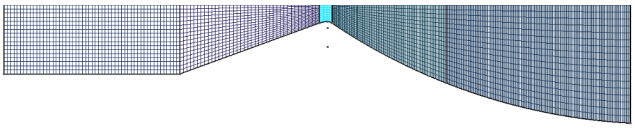

(b) Mesh with 11560 elements.

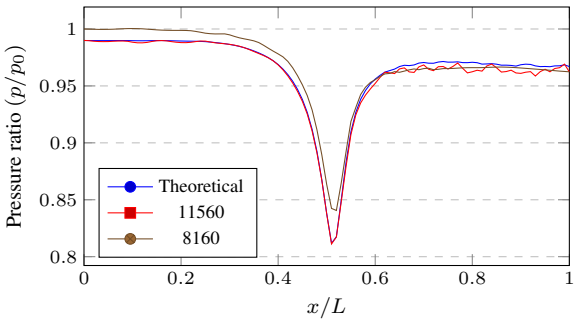

(c) Comparative result between two different meshes.

Figure 4. The effect of the number of elements in the solution.

Once the mesh quality was assured, the simulation phase of different conditions in the nozzle was tested. Remember that the rocket engine will be efficient if, and only if, the flow reaches speeds higher than the sound, however it is known that this does not always happen. There are some conditions which make it impossible to accelerate the flow, for example the pressure ratio adopted between the upstream and downstream sections.

Three important situations were analyzed. They are: subsonic, supersonic flow with shock wave (irreversible process) and supersonic flow (reversible idealization of optimized flow).

All the simulations performed were monitored and showed residual error in the order of 10^{-8} (see the following cases), which guarantees a good convergence of the numerical method. Already the accuracy was inferred from the comparison between the numerical result and the expected theory.

3.1 Subsonic flow

By setting an inlet pressure while altering the downstream pressure, it is possible to vary the flow rate. In this context, we use a pressure ratio of 0.89 between upstream and downstream section.

Regarding the aspect of convergence, i.e., how accurate the solution is, during the solution process the residue (difference between the solution found in a given iteration and the previous iteration) was monitored to ensure a sufficiently low value.

In Fig 5 shows the value of the residue obtained, which is of the order of 10^-8 for the monitored properties.

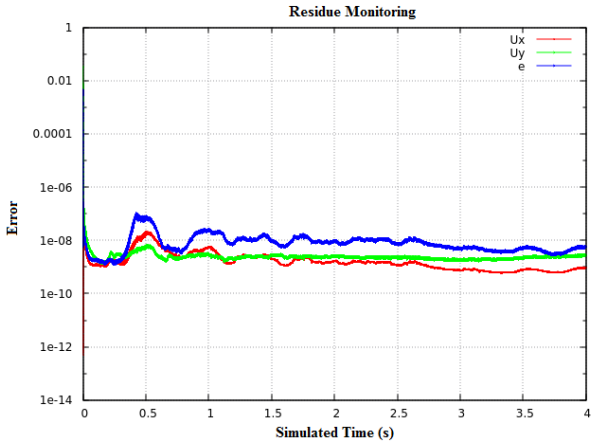

Figure 5. Residue obtained for the subsonic case.

Since low residue values represent good convergence and ensure that the conservation equations were solved with a small error, flow field analysis was performed.

In performing the comparative analysis (Fig.6 and Fig.7), it was found that the numerical results for the properties of the flow field match the expected result from the theoretical point of view.

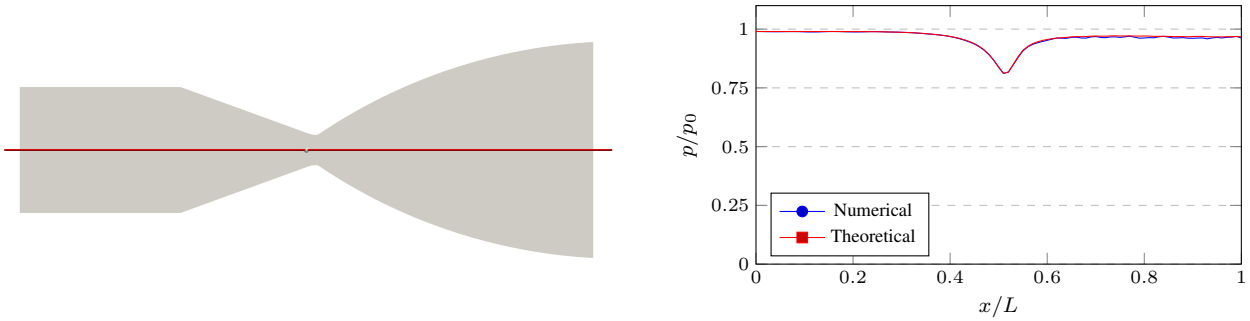

(a) Reference line supported for numerical solution. (b) Numerical vs Theoretical Result for pressure ratio.

Figure 6. Validation for the subsonic case.

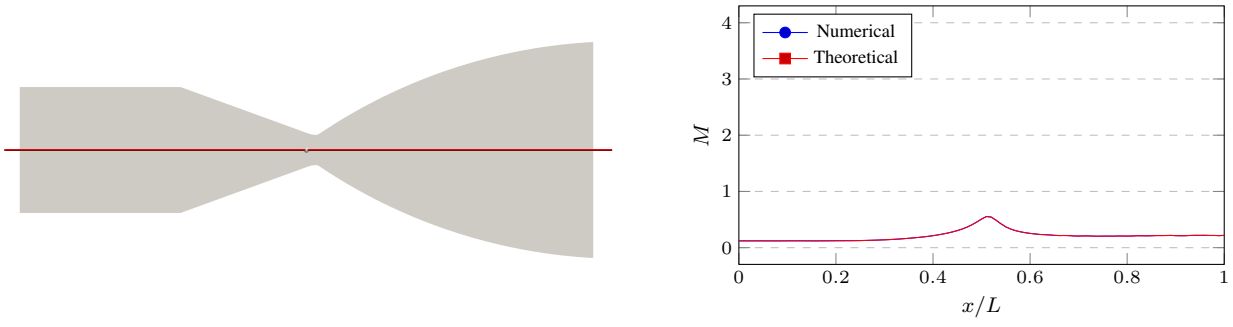

(a) Reference line supported for numerical solution. (b) Numerical vs Theoretical Result for speed.

Figure 7. Validation for the subsonic case.

The detailed results are presented below:

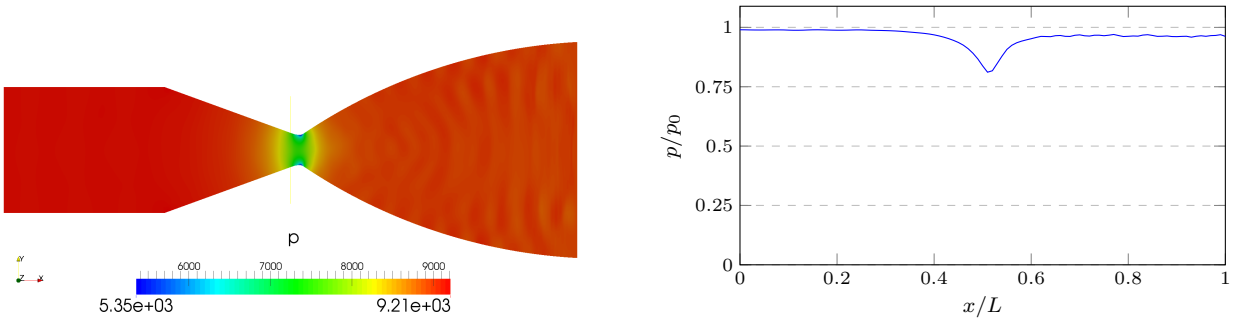

(a) Distribution of pressures inside the nozzle. (b) Pressure variation inside the nozzle.

Figure 8. Behavior of the pressure for the subsonic case.

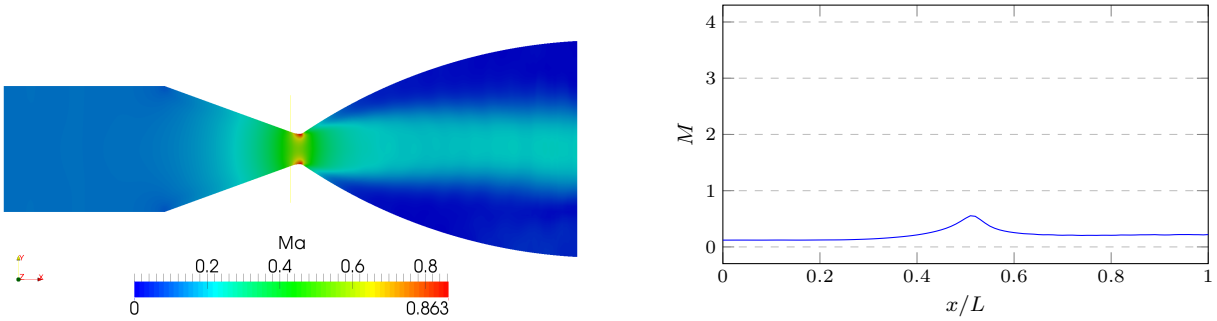

(a) Flow variation in terms of Mach. (b) Numerical result.

Figure 9. Mach number for a subsonic flow.

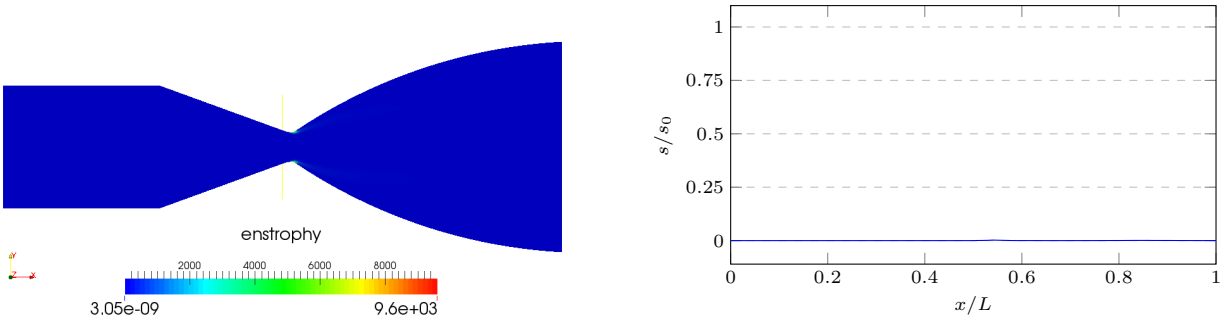

(a) Distribution of the entropy range. (b) Variation of entropy inside the nozzle. Shock no present.

Figure 10. Behavior of the entropy variation for the subsonic case.

By analyzing the pressure behavior (Fig.8), it is seen that the pressure decreases in the converging section and in counterpart as it reaches the CD nozzle throat the pressure begins to increase in the diffuser.

See in the Fig.9.b that the flow is accelerated in the convergent nozzle, but the pressure ratio is not enough for the flow to reach the sonic velocity in the throat, so upon reaching the diffuser the flow is decelerated.

From the Fig.9.a we see the highest Mach concentrated at the edges of the throat and the velocity in the divergent concentrated in the middle. This apparent separation in the divergent, with almost null at the edges, may be due to numerical dissipation.

In the case of subsonic flow, theren't will be an internal irreversibilities on the CD nozzle. See in the Fig.10 that the flow is isentropic along the device.

3.2 Supersonic flow with shock waves

Unlike the previous case, the pressure ratio used here is sufficient to accelerate the flow until a critical Mach ($M = 1$) is obtained in the nozzle throat.

The procedures for obtaining the numerical results consisted of analyzing the device subject to a pressure variation of $0,35$. The simulation time was $4s$, sufficient for the simulation residue to be less than 10^-8, as shown in Fig.11.

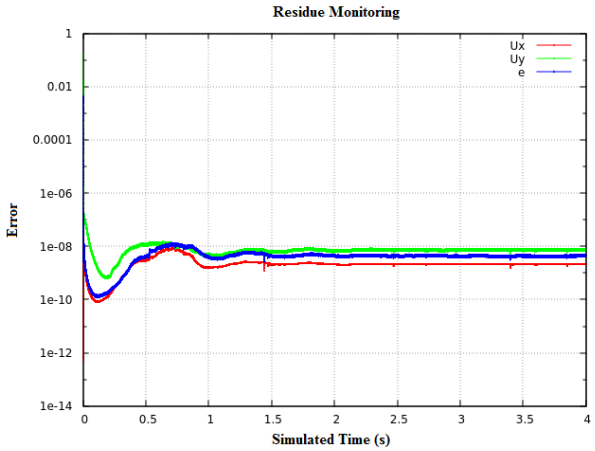

Figure 11. Residue obtained for the supersonic case with shock waves.

The pressure ratio curves for the numerical and theoretical solution (Fig.12) and for the Mach number (Fig.13). The relative deviation associated with the supersonic case along the entire nozzle was less than 5% except where the shock occurred, at this point the value was 35%.This value is associated with the mesh used.

As the shock wave has a micrometric thickness a more refined mesh will more accurately guarantee the deviation at each point in the flow field.

(a) Reference line supported for numerical solution.

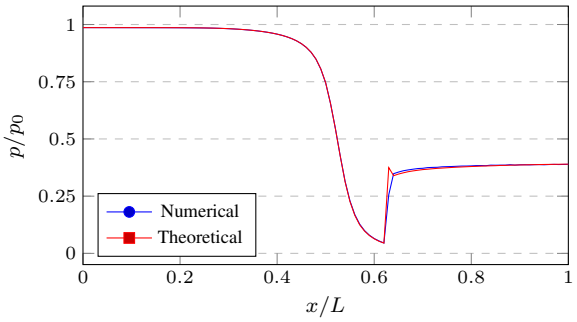

(b) Numerical vs Theoretical Result for pressure ratio.

Figure 12. Validation for the subsonic case with the presence of irreversibilities, pressure effect.

(a) Reference line supported for numerical solution.

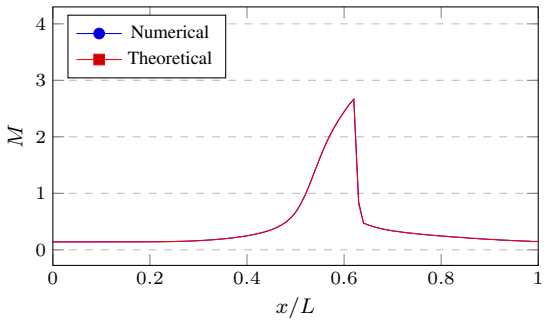

(b) Numerical vs Theoretical Result for speed.

Figure 13. Validation for the subsonic case with the presence of irreversibilities, velocity effect.

The detailed results are presented below:

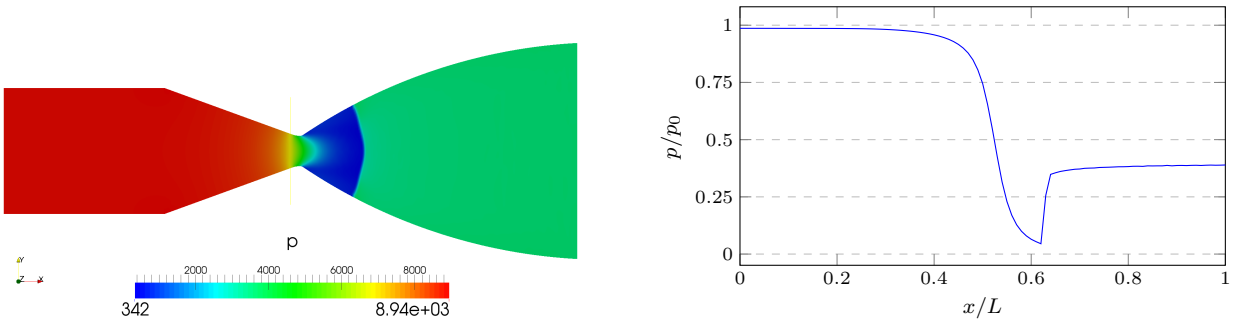

(a) Distribution of pressure inside the nozzle. (b) Pressure variation inside the nozzle.

Figure 14. Behavior of the pressure for the supersonic case with the presence of irreversibilities.

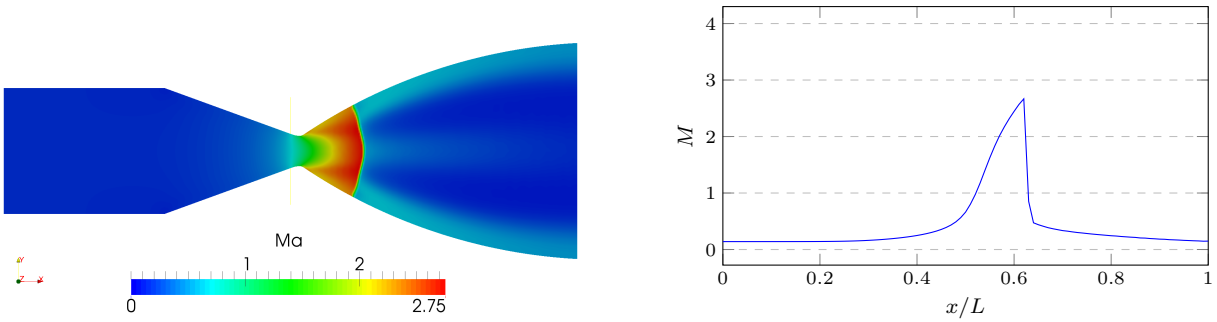

(a) Flow variation in terms of Mach. (b) Numerical result.

Figure 15. Mach number for a supersonic flow.

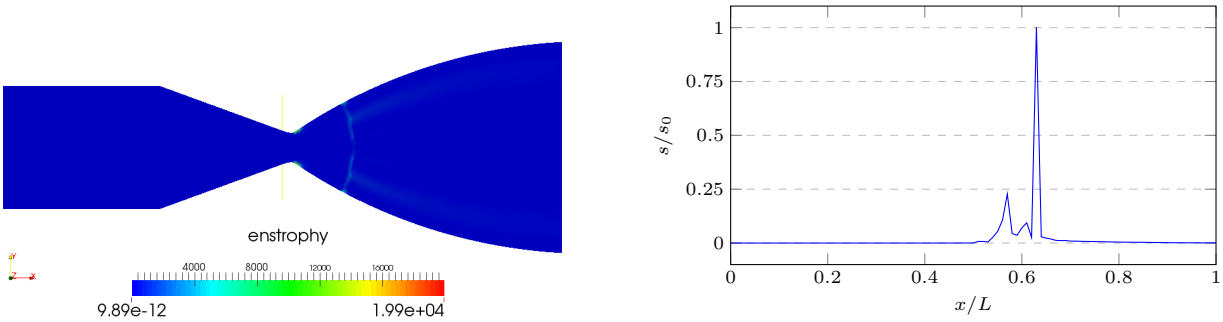

(a) Distribution of the entropy range. (b) Variation of entropy inside the nozzle. Shock present.

Figure 16. Behavior of the entropy variation for the supersonic case with the presence of irreversibility.

From the Fig.14, it is noticed that after the constant decrease of the pressure as the flow passes through the convergent section, occurs in the divergent section a discontinuity followed by a sudden increase of the pressure due to the presentation of the shock wave.

Analyzing Fig.15 note that flow is accelerated in both the convergent and divergent nozzles. However, when the diffuser is subjected to the irreversible phenomenon characterized by a sudden decrease in velocity, the irreversibility is so intense that it causes the supersonic flow to have its speed reduced instantly.

In Fig.15.a the shock wave structure is non-flat and shows the characteristic $2D$ of the supersonic flow after the throat. Apparently the shock is not normal near the walls, since it seems not to have fallen below $Ma = 1$.

Note in Fig.16 that the flow is isentropic along almost the entire nozzle, except for the region where the shock wave occurs. In this small region the entropy variation is maximal. There is a large dissipation of energy to compensate for the choice of an unsatisfactory pressure ratio that resulted in the adverse pressure gradient.

3.3 Ideal supersonic flow

It is the design curve, ideal condition of operation of the rocket motor where no irreversibility will be present to prevent the continuous acceleration of the fluid. Consequently it is possible to obtain high values of Mach and a great thrust. Such condition was obtained using a pressure ratio of $0,02$.

The residue was monitored during the simulation of $4s$, sufficient time to obtain a residue less than 10^-8, as shown in Fig.17.

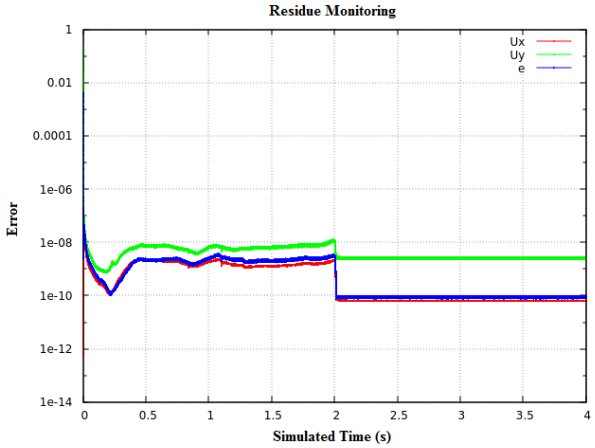

Figure 17. Residue obtained for the supersonic case without shock waves.

All graphs referring to the present case were obtained by reference to the centerline (Fig.18.a) and (Fig.19.a). After analysis, it was found that the simulation showed a relative error between the numerical and theoretical results of less than 5% (Fig.18.b and Fig.19.b).

(a) Reference line supported for numerical solution.

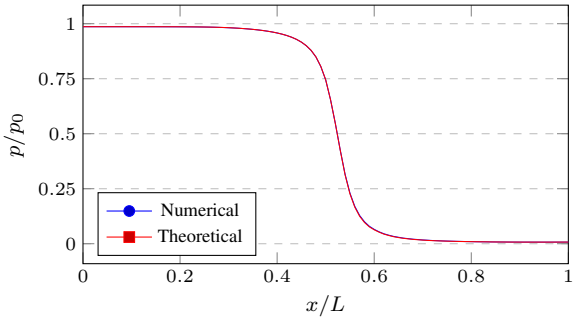

(b) Numerical vs Theoretical Result for pressure ratio.

Figure 18. Validation for the supersonic case without the presence of irreversibilities, pressure effect.

(a) Reference line supported for numerical solution.

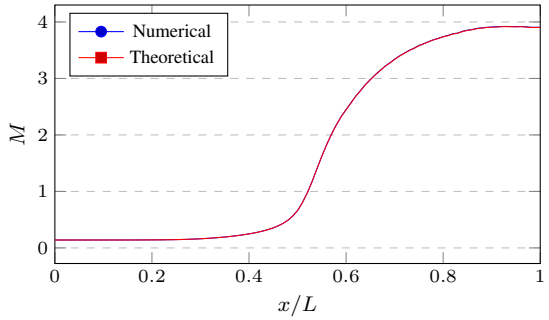

(b) Numerical vs Theoretical Result for speed.

Figure 19. Validation for the supersonic case without the presence of irreversibilities, velocity effect.

The detailed results are presented below:

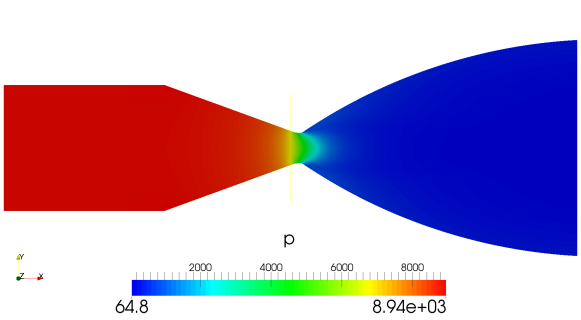

(a) Ideal pressure distribution inside the nozzle.

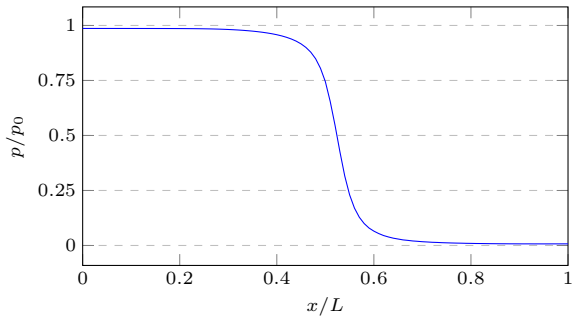

(b) Pressure variation inside the nozzle.

Figure 20. Behavior of the pressure for the supersonic case without the presence of irreversibility.

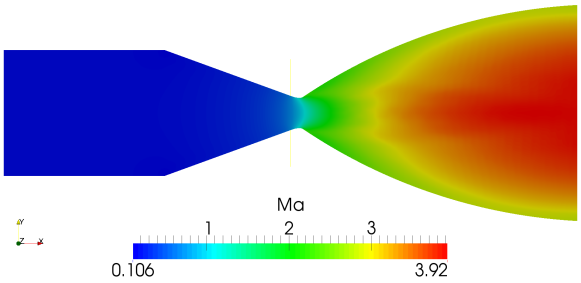

(a) Flow variation in terms of Mach.

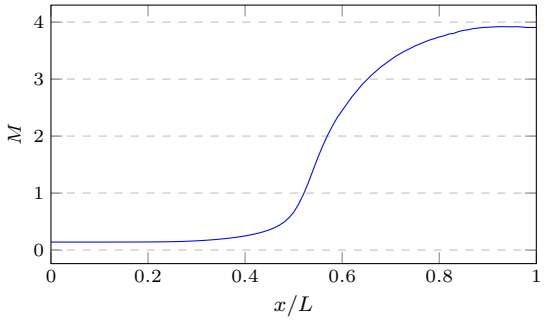

(b) Numerical result.

Figure 21. Mach number for a ideal supersonic flow.

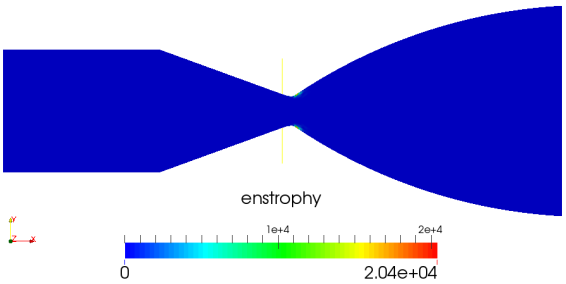

(a) Distribution of the entropy range.

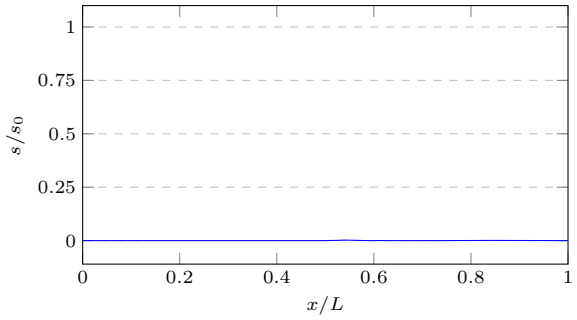

(b) Variation of entropy inside the nozzle. Shock no present.

Figure 22. Behavior of the entropy variation for the supersonic case without the presence of irreversibility.

Notice in Fig.20 that the pressure ratio decrease while the flow velocity increases continuously by presenting its maximum value at the outlet of the nozzle (Fig.21). Note also the characteristic $2D$ of the simulation, but that the results may be suffering from numerical dissipation of the model used near the walls again.

3.4 Effect of pressure ratio

See Fig.23 and Fig.24 for the behavior of the flow in the rocket motor for the Pressure and Mach operating at various back pressures. This results are analogous to the presented in literature by Fox *et al.* (2000), Cengel and Cimbala (2015), Young and Okiishi (2004) and White (2010).

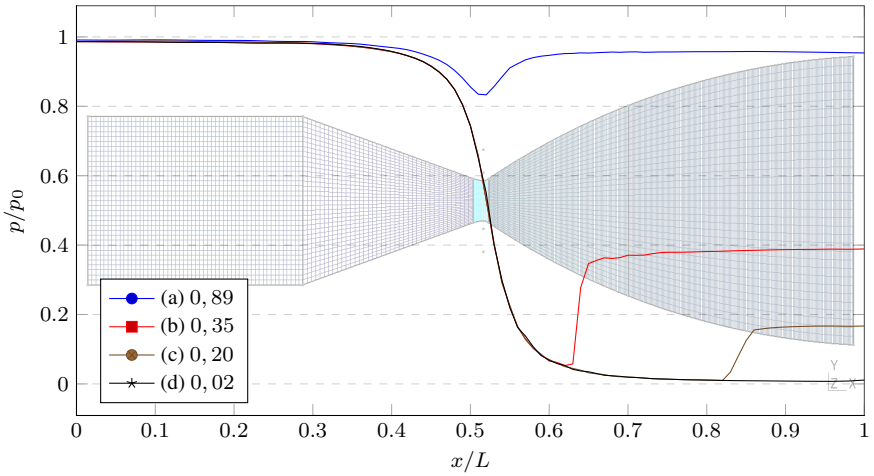

Figure 23. Behavior of the rocket engine for the pressure operating at various backpressures.

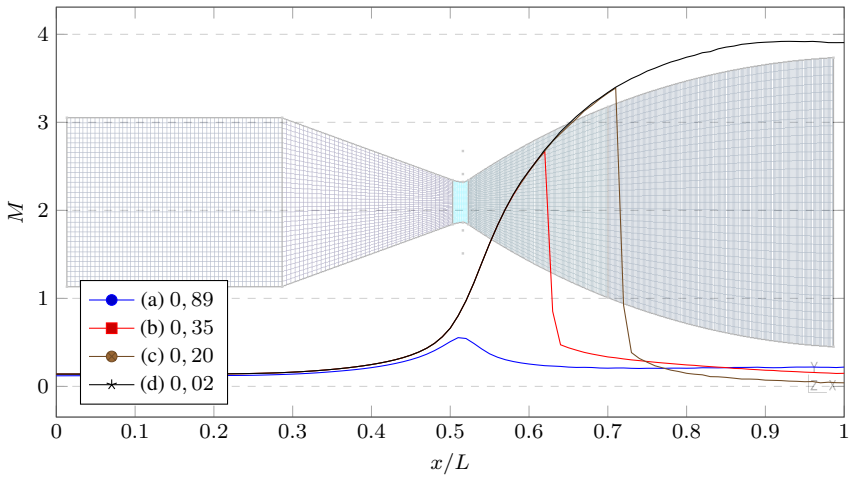

Figure 24. Behavior of the rocket engine for the Mach operating at various backpressures.

If the back pressure is reduced further (a) the flow increases and consequently the velocity will also increase in the converging section.

Still in case (b) the flow reaches the critical velocity in the throat of the nozzle, so when traversing the divergent section it is possible to continue accelerating. However, there is an irreversible phenomenon called shock wave, which results in energy dissipation in order to compensate for the adverse pressure gradient between the inlet and outlet section of the nozzle.

Notice in case (b), the abrupt increase in pressure (Fig.23) resulting in the immediate drop in speed (Fig.24). Since the speed is reduced to subsonic levels in the diffuser, the speed will continue to decrease until the outlet of the nozzle.

Finally, note in Fig.23 and Fig.24 that it is possible to displace the shock wave downstream by reducing the pressure ratio. Shifting the shock wave downstream of the nozzle implies a higher velocity, achieved moments before the onset of the shock wave (case c).

By further reducing the pressure (case d) the ideal flow condition is achieved, characterized by absence irreversivity, maximum flow velocity, and consequently the maximum rocket engine thrust force.

There are situations where the shock wave stops being a normal wave and becomes oblique waves, that occurs outside the nozzle.

The curves in Fig.23 and Fig.24 shown clearly demonstrate the care engineers of rocket motors must have with the conditions of the rocket motor. It is essential to monitor the expansion gases maintaining a suitable pressure ratio to maximize flow and thrust force.

4. CONCLUSIONS

The methodology described here, allowed to obtain an approximate prediction of the behavior that will be observed when applying certain pressure ratios in a CD nozzle. The study successfully demonstrated the two-dimensional flow behavior. The characteristic curves obtained for the 2D flow match with results presented in the literature for the quasi unidimensional flow.

After successive numerical simulations involving different meshes and different pressure ratios between the inlet and outlet sections of the nozzle, it was observed the need to use an appropriate ratio to reach the maximum thrust force, since insufficient pressure ratios result in subsonic speeds in the outlet of the nozzle as a result of the flow not reaching the sonic velocity in the throat of the nozzle, or due to the appearance of irreversibility which result in strong shock waves.

The understanding of these results will allow to implement improvements in new numerical analyzes involving the variables of the flow. In addition, it will serve as the initial condition for experiments containing this Laval nozzle design.

5. REFERENCES

Anderson, J.D., 1990. *Modern compressible flow: with historical perspective*, Vol. 12. McGraw-Hill New York.

Anderson, J.D., 2001. *Fundamentals of aerodynamics*. McGraw-Hill New York.

Cengel, Y.A. and Cimbala, J.M., 2015. *Mecânica dos fluidos - 3ª Edição*. AMGH Editora.

Einfeldt, B., 1988. "On godunov-type methods for gas dynamics". *SIAM Journal on Numerical Analysis*, Vol. 25, No. 2, pp. 294–318.

Fernandes, L., Freitas, R., Mendonca, M., Flatschart, R. and Pantaleão, A., 2012. "Numerical simulation of film cooling with auxiliary holes". In *50th AIAA Aerospace Sciences Meeting including the New Horizons Forum and Aerospace Exposition*. p. 327.

Fernandes, L.M., 2012. *Estudo computacional de configurações de resfriamento por filme em turbinas a gás*. Master's thesis, Instituto Tecnológico de Aeronáutica.

Fox, R.W., Pritchard, P.J. and McDonald, A.T., 2000. *Introdução À Mecânica Dos Fluidos* . Grupo Gen-LTC.

Freitas, P., 2014. *Numerical simulation of compressible flow over a deep cavity*. Ph.D. thesis, Master Thesis. Técnico Lisboa.

Godunov, S., 1959. "A finite difference method for the computation of discontinuous solutions of the equations of fluid dynamics." *Sbornik: Mathematics*, Vol. 47, No. 8-9, pp. 357–393.

Gupta, A., 2016. "Shock tube with rhocentralfoam, sonicfoam, lax-friedrichs and maccormacks".

Lantz, R. *et al.*, 1971. "Quantitative evaluation of numerical diffusion (truncation error)". *Society of Petroleum Engineers Journal*, Vol. 11, No. 03, pp. 315–320.

Salvador, N.M.C., 2005. *Simulação nuérica do escoamento em um motor foguete com reação química*. Ph.D. thesis.

White, F.M., 2010. *Mecânica dos Fluidos - 6ª Edição*. AMGH Editora.

Young, D. and Okiishi, T., 2004. "Fundamentos da mecânica dos fluidos". *Tradução da 4ª edição norte-americana. Edgard Blucher*.

6. RESPONSIBILITY NOTICE

The author(s) is (are) the only responsible for the printed material included in this paper.